Available online at www.sciencedirect.com
ScienceDirect
Polymer Degradation and Stability 92 (2007) 1265–1278
Polymer Degradation and Stability
www.elsevier.com/locate/polydegstab

Thermal degradation behaviors of polybenzoxazine and silicon-containing polyimide blends

Sunan Tiptipakorn [a], Siriporn Damrongsakkul [a], Shinji Ando [b], Kasinee Hemvichian [c], Sarawut Rimdusit [a,*]

[a] *Department of Chemical Engineering, Faculty of Engineering, Chulalongkorn University, Pathumwon, Bangkok 10330, Thailand*
[b] *Department of Chemistry and Material Sciences, Graduate School of Science and Engineering, Tokyo Institute of Technology, Ookayama, Meguro-ku, Tokyo 152-8552, Japan*
[c] *Chemistry and Material Science Research Program, Office of Atoms for Peace, 16 Vibhavadi Rangsit Road, Chatuchak, Bangkok 10900, Thailand*

Received 4 December 2006; received in revised form 20 March 2007; accepted 22 March 2007
Available online 14 April 2007

Abstract

Thermal behaviors of polymer blends between common-type polybenzoxazine (PBA-a) and polysiloxane-*block*-polyimide (SPI) were studied using Dynamic Mechanical Analysis (DMA) and Thermogravimetric Analysis (TGA). The polymer blends showed only one glass-transition temperature (T_g) that increased as the content of SPI increased. Synergistic behavior in the char formation of the alloys was clearly observed. The DTG curves showed three stages and two stages of decomposition reaction in neat PBA-a and SPI, respectively. For the blending systems with 25 wt%, 50 wt%, and 75 wt% of SPI, the DTG thermograms of the blends exhibited four stages of thermal decomposition reaction. The apparent activation energies (E_a) of each step were determined using Kissinger method, Flynn–Wall–Ozawa method and Coats–Redfern method. The type of solid state mechanism was determined by Criado method. From the calculation, the solid state thermal degradation mechanism is proposed to be F1 (random nucleation with one nucleus on the individual particle) type for PBA-a, SPI, and their blends.

Keywords: Polybenzoxazine; Silicon-containing polyimide; Kinetics; Degradation; Char yield

1. Introduction

Polymer blends between polybenzoxazines and other polymers have been a subject of many current investigations, which aim to utilize some outstanding properties of polybenzoxazines. Polybenzoxazines are particularly applied to improve the processability, mechanical, and adhesion properties of the resulting resin mixtures. They can be synthesized via a simple and cost-competitive solventless technology [1]. Moreover, their molecular design flexibility provides wide range of properties that can be tailor-made. The polymers have been reported to possess many intriguing properties such as high mechanical properties, high char yield, near zero shrinkage, low water absorption, excellent electrical properties, low melt viscosity, self-polymerized upon heating, and no by-products during curing [2].

Although there were many studies about this family of the polymers, little is known about the thermal degradation of polybenzoxazine. Hemvichian et al. [3] studied the degradation process of polybenzoxazine in common type (PBA-a) by using TGA and GC–MS. They identified the structures of pyrolysis products. However, the solid state thermal degradation mechanism and kinetics study of PBA-a have not been studied before.

In general, the approaches for improving the performance of polybenzoxazine can be classified into two ways. One is

* Corresponding author. Tel.: +66 2 218 6862; fax: +66 2 218 6877.
E-mail address: sarawut.r@chula.ac.th (S. Rimdusit).

0141-3910/$ - see front matter © 2007 Elsevier Ltd. All rights reserved.
doi:10.1016/j.polymdegradstab.2007.03.021

the structure modification of benzoxazine monomers; the other is the formation of composites or blends with other high-temperature polymers like polyimide [4] as well as with inorganic fillers such as clay [5] and metal oxide [6]. The blend of polysiloxane-*block*-polyimide (SPI) is proposed to enhance the PBA-a properties in this study.

Many researches [7–9] revealed that polysiloxane-*block*-polyimide (SPI) has a number of attractive characteristics, i.e. low moisture sorption, excellent thermal stability, and lower dielectric constant. Furthermore, this kind of block copolymer is reported to increase the flexibility of the materials. Therefore, the thermal degradation of the blends between polybenzoxazine and polysiloxane-*block*-polyimide (SPI) is worthy to investigate.

In this research, we prepared polymer blends of PBA-a and SPI. The glass-transition temperatures and thermal characteristic were determined by Differential Scanning Calorimetry (DSC), Dynamic Mechanical Analysis (DMA), and Thermal Gravimetric Analysis (TGA). The thermal degradation kinetic parameters, activation energy (E_a) and pre-exponential factor (A), were evaluated by using three well-known methods, i.e. Kissinger method, Flynn–Wall–Ozawa method, and Coats–Redfern method. Kissinger method and Flynn–Wall–Ozawa method were used in this study because they are mostly used in the literatures and can be used without prior knowledge of reaction mechanism. Additionally, Coats and Redfern method was used because it renders the degradation parameters such as E_a, A, and possible reaction mechanism. The thermal degradation mechanism of PBA-a, SPI, and the blend was also evaluated by using Criado method.

2. Theoretical consideration

Generally for polymer degradation, it is assumed that the rates of conversion are proportional to the concentration of reacted material. The rate of conversion can be expressed by the following basic rate equation

$$\frac{d\alpha}{dt} = kf(\alpha) \tag{1}$$

For thermogravimetric analysis, the fraction of decomposition (α) is defined as the ratio of weight loss at time t to total weight loss at complete decomposition temperature as shown in Eq. (2).

$$\alpha = \frac{(M_o - M_t)}{(M_o - M_f)} \tag{2}$$

where M_t is the weight of the sample at time t; M_o is the initial weight of the sample and; M_f is the final weight of the completely decomposed sample.

It is assumed that k follows the Arrhenius equation.

$$k = A\exp(-E_a/RT) \tag{3}$$

Substituting "k" from Eq. (3) into Eq. (1) one obtains:

$$\frac{d\alpha}{dt} = A\exp(-E_a/RT)f(\alpha) \tag{4}$$

According to non-isothermal kinetic theory, thermal degradation at a constant heating rate, β

$$\beta = dT/dt \tag{5}$$

can be expressed by Eq. (6)

$$\frac{d\alpha}{dT} = \frac{A}{\beta}\exp(-E_a/RT)f(\alpha) \tag{6}$$

where $f(\alpha)$ is the differential expression of a kinetic model function, α is the conversion, β is the heating rate (K min^{-1}), E_a and A are the so-called activation energy (kJ/mol) and pre-exponential factor (min^{-1}) for the decomposition reaction, respectively. R is the gas constant (8.314 J mol^{-1} K^{-1}).

Generally, E_a can be calculated by using three well-known methods for dynamic heating experiment, i.e. Kissinger method, Flynn–Wall–Ozawa method, and Coats–Redfern method [10–12].

2.1. Kissinger method (differential method) [12–15]

Kissinger method uses Eq. (7) to determine the E_a of solid state reactions.

$$\ln\left(\frac{\beta}{T_P^2}\right) = \ln\frac{AR}{E_a} + \ln\left[n\left(1-\alpha_p\right)^{n-1}\right] - \frac{E_a}{RT_p} \tag{7}$$

where T_p and α_p are the absolute temperature and weight loss at maximum weight-loss rate $(d\alpha/dt)_p$, respectively, and n is the reaction order. From the slope of the straight line $\ln(\beta/T_p^2)$ versus $1/T_p$, the E_a can be obtained. The advantage of the Kissinger model is that the E_a can be obtained without the knowledge of any thermal degradation reaction mechanism in advance.

2.2. Flynn–Wall–Ozawa method (integration method) [11–16]

Flynn–Wall–Ozawa method can be employed to quantify E_a without any knowledge of the reaction mechanisms. The main advantage of this method is that it is not based on any assumption concerning the temperature integral, giving, thus, a higher degree of precision to the results.

From Eq. (6), it can be integrated using the Doyle approximation [17,18]. The result of the integration after taking logarithms is

$$\log\beta = \log\frac{AE_a}{g(\alpha)R} - 2.315 - \frac{0.457E_a}{RT} \tag{8}$$

The E_a of the thermal degradation process of the blending system was determined from the slope of the straight line $\log\beta$ versus $1/T$.

2.3. Coats–Redfern method [10,11,23]

Besides the above two methods, Coats–Redfern method is often used in kinetic analysis of solid state processes. Coats–Redfern method is presented in Eq. (9).

$$\ln\frac{g(\alpha)}{T^2} = \ln\left(\frac{AR}{\beta E_a}\right) - \frac{E_a}{RT} \tag{9}$$

From the slope of the straight line $\ln[(g(\alpha))/T^2]$ versus $1/T$, E_a can be calculated and A can be obtained from the intercept, i.e. from $\ln(AR/\beta E_a)$.

2.4. Criado method [19–21]

The degradation reaction mechanism can be determined using Criado method [19]. Criado et al. [19] proposed a method which can accurately determine the reaction mechanism in the solid reaction process.

Criado et al. defined a type of $Z(\alpha)$ function

$$Z(\alpha) = \frac{\left(\frac{d\alpha}{dt}\right)}{\beta}\pi(x)T \tag{10}$$

where $x = E_a/RT$ and $\pi(x)$ is an approximate expression obtained by integration against temperature, which cannot be expressed by simple analysis formulas, Paterson [22] proposed a reasonable relationship between $\pi(x)$ and $P(x)$ as shown in Eq. (11).

$$\pi(x) = x\,e^x P(x) \tag{11}$$

Senum and Yang [23] proposed the fourth rational expression of $P(x)$

$$P(x) = \frac{e^{-x}}{x}\frac{x^3 + 18x^2 + 86x + 96}{x^4 + 20x^3 + 120x^2 + 240x + 120} \tag{12}$$

when $x > 20$, the error of Eq. (15) is less than $10^{-5}\%$, which is the basis we use in this paper.

Combining Eqs. (1), (10) and (11), we can obtain:

$$Z(\alpha) = f(\alpha)g(\alpha) \tag{13}$$

From Eqs. (1), (10) and (11), the following relationship can be derived:

$$Z(\alpha) = \frac{d\alpha}{dT}\frac{E_a}{R}e^{E_a/RT}P(x) \tag{14}$$

Eq. (13) is used to plot the master $Z(\alpha)$–α curves for different models listed in Table 1 [24], whereas Eq. (14) is used for representing the experimental curve. By comparing these two curves, the mechanism type of the thermal degradation can be identified.

3. Experimental

3.1. Materials

The benzoxazine monomer bis(3-phenyl-3,4-dihydro-2*H*-1,3-benoxzinyl) isopropane (BA-a) as shown in Fig. 1a was prepared from 2,2′-bis(4-hydroxyphenyl)-propane (Bisphenol-A) with aniline and formaldehyde according to the reported method [25]. Bisphenol-A (commercial grade) provided by Thai Polycarbonate Co., Ltd. (TPCC) was used as received. Para-formaldehyde (AR grade) and aniline (AR grade) were purchased from Merck and APS Finechem Companies. As shown in Fig. 1b, polysiloxane-*block*-polyimide (SPI) under the trademark of ''BSF30'' with molecular weight of 167,720 was obtained from Nippon Steel Chemical. The ratio of the block components (polysiloxane/polyimide) is 36.8 mol%.

3.2. Synthesis of blends

Polysiloxane-*block*-polyimide (SPI) was blended with benzoxazine monomers at various weight ratios, i.e. 100:0, 75:25, 50:50, 25:75, and 0:100. The blends were formed in a Teflon mould and dried at 60 °C for 18 h. After that, the thermal treatment was performed at 100 °C (for 1 h), 150 °C (for 1 h), and 200 °C (for 4 h) in a vacuum oven.

Table 1
Algebraic expressions for $g(\alpha)$ and $f(\alpha)$ for the most frequently used mechanisms of solid state processes

Mechanism	$g(\alpha)$	$f(\alpha)$
A_2, Nucleation and growth (Avrami equation (1))	$[-\ln(1-\alpha)]^{1/2}$	$2(1-\alpha)[-\ln(1-\alpha)]^{1/2}$
A_3, Nucleation and growth (Avrami equation (2))	$[-\ln(1-\alpha)]^{1/3}$	$3(1-\alpha)[-\ln(1-\alpha)]^{2/3}$
A_4, Nucleation and growth (Avrami equation (3))	$[-\ln(1-\alpha)]^{1/4}$	$4(1-\alpha)[-\ln(1-\alpha)]^{3/4}$
R_1, Phase boundary controlled reaction (one-dimensional movement)	α	1
R_2, Phase boundary controlled reaction (contracting area)	$[1-(1-\alpha)^{1/2}]$	$2(1-\alpha)^{1/2}$
R_3, Phase boundary controlled reaction (contracting volume)	$[1-(1-\alpha)^{1/3}]$	$3(1-\alpha)^{2/3}$
D_1, One-dimensional diffusion	α^2	$(1/2)\alpha^{-1}$
D_2, Two-dimensional diffusion (Valensi equation)	$(1-\alpha)\ln(1-\alpha)+\alpha$	$-[\ln(1-\alpha)]^{-1}$
D_3, Three-dimensional diffusion (Jander equation)	$[1-(1-\alpha)^{1/3}]^2$	$(3/2)[1-(1-\alpha)^{1/3}]^{-1}(1-\alpha)^{2/3}$
D_4, Three-dimensional diffusion (Ginstling Brounshtein equation)	$[1-(2/3)\alpha]-(1-\alpha)^{2/3}$	$(3/2)[1-(1-\alpha)^{1/3}]^{-1}$
F_1, Random nucleation with one nucleus on the individual particle	$-\ln(1-\alpha)$	$1-\alpha$
F_2, Random nucleation with two nuclei on the individual particle	$1/(1-\alpha)$	$(1-\alpha)^2$
F_3, Random nucleation with three nuclei on the individual particle	$1/(1-\alpha)^2$	$(1/2)(1-\alpha)^3$

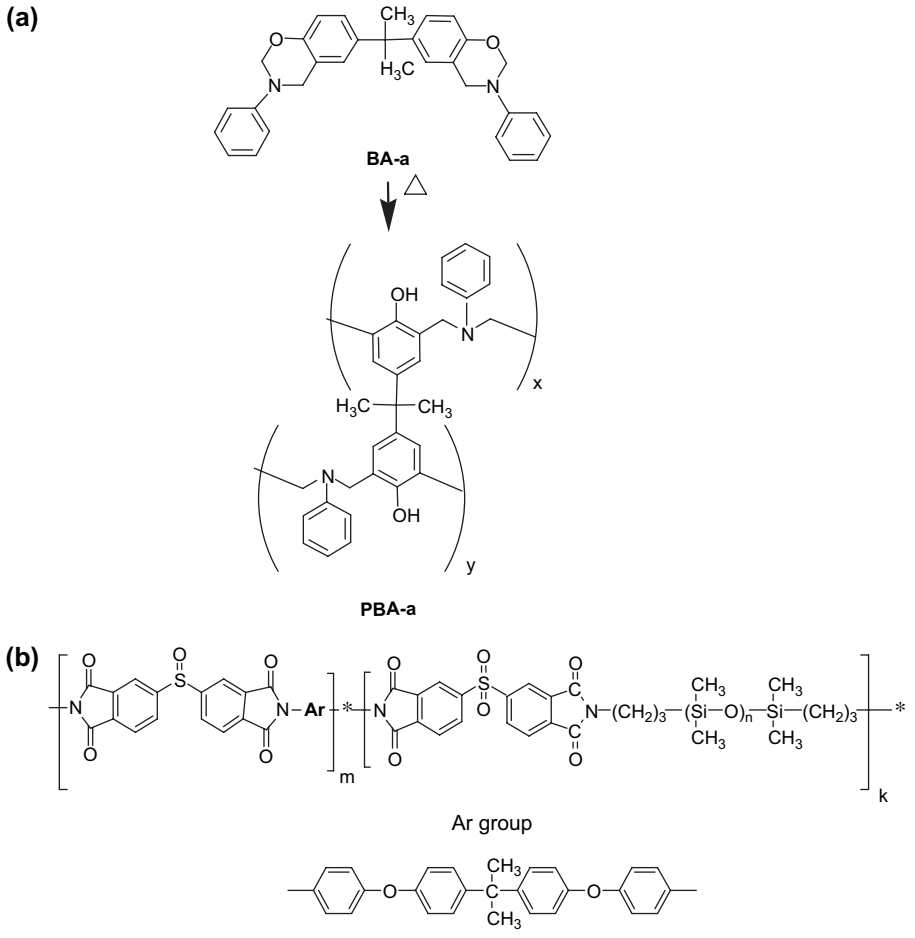

Fig. 1. (a) Benzoxazine monomer and polybenzoxazine; (b) polysiloxane-*block*-polyimide (SPI).

4. Measurements

4.1. Thermal analysis

Differential Scanning Calorimeter (DSC) of TA instruments (model DSC2910), calibrated with Indium standard, was used. A sample of about 10 mg was used for each test. In order to erase any thermal history, the samples were heated at 10 °C/min. Then, they were cooled to the ambient temperature, and scanned again using the same heating rate as before.

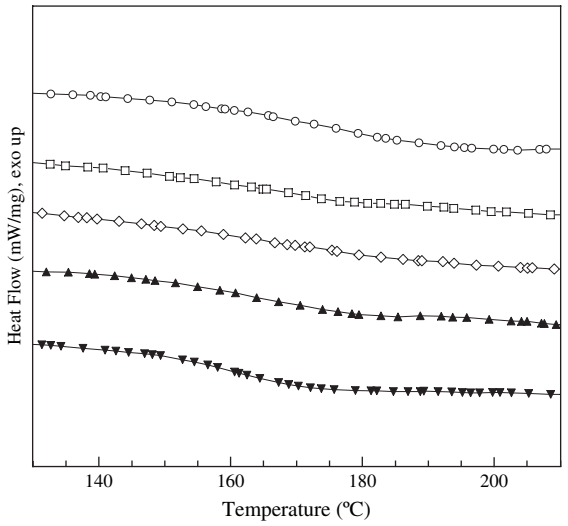

Fig. 2. DSC thermograms of PBA-a, SPI and their blends at various SPI contents: (○) SPI, (□) 75 wt%, (◇) 50 wt%, (▲) 25 wt%, and (▼) PBA-a.

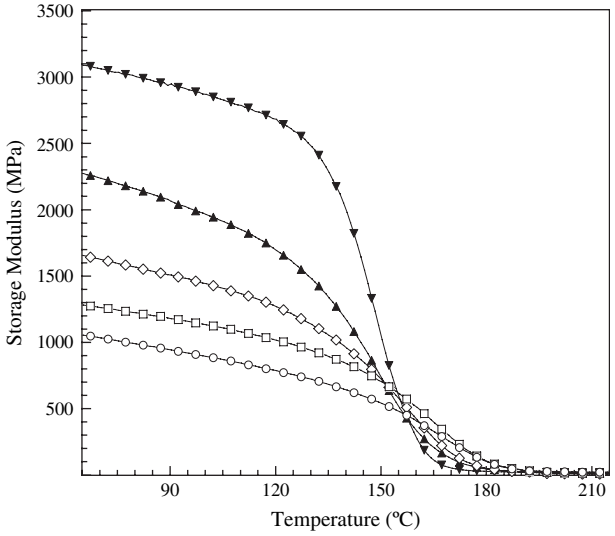

Fig. 3. Storage moduli of PBA-a, SPI and their blends at various SPI contents: (○) SPI, (□) 75 wt%, (◇) 50 wt%, (▲) 25 wt%, and (▼) PBA-a.

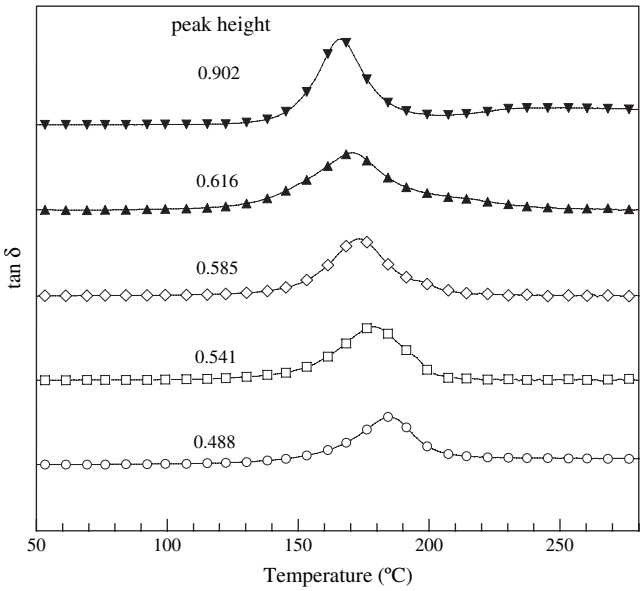

Fig. 4. Loss tangent of PBA-a, SPI and their blends at various SPI contents: (○) SPI, (□) 75 wt%, (◇) 50 wt%, (▲) 25 wt%, and (▼) PBA-a.

The glass-transition temperatures (T_g) of the blends were measured.

Dynamic mechanical properties of the blends were tested using the NETZSCH Model DMA242. The experiment is done in a tension mode using the dimension of the specimens of approximately 23.7 mm (length) × 5 mm (width) × 0.5 mm (thickness). The applied strain amplitude was 0.3% at the deformation frequency of 1 Hz. The specimens were heated using a temperature ramp rate of 3 °C/min from 40 to 250 °C.

4.2. Thermal gravimetric analysis (TGA)

The decomposition temperature (T_d) and char yield of the blends were studied using TGA Instruments (model TGA/SDTA 851[e]). The experiments were performed using a heating rate of 20 °C/min from 40 to 1000 °C under nitrogen atmosphere. The flow of purging nitrogen was kept at 80 ml/min. The sample mass was approximately 20 mg.

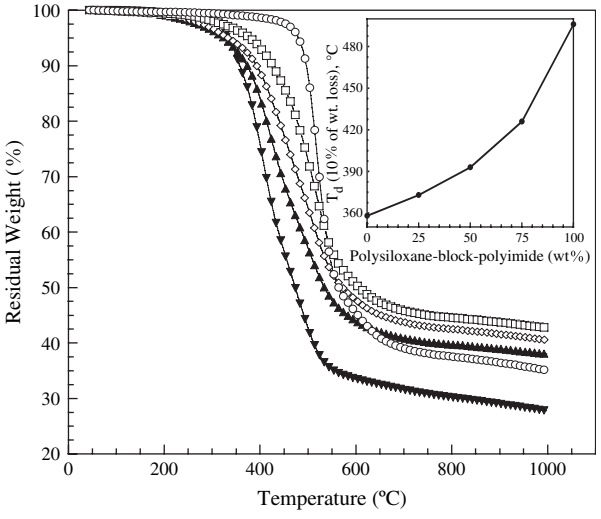

Fig. 5. Thermogravimetric curves of PBA-a, SPI and their blends at various SPI contents: (○) SPI, (□) 75 wt%, (◇) 50 wt%, (▲) 25 wt%, and (▼) PBA-a. Inset: decomposition temperatures (T_d at 10% weight loss) at various SPI contents.

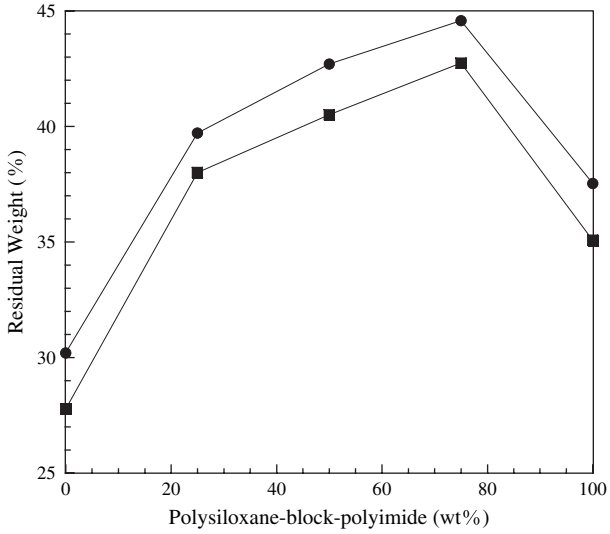

Fig. 6. Char yield of PBA-a, SPI and their blends at various temperatures: (●) 1000 °C, (■) 800 °C.

Kinetics analysis via Kissinger method, Flynn–Wall–Ozawa method, and Coats–Redfern method was carried out at various heating rates, i.e. 5, 10, 20, and 25 °C/min.

5. Results and discussion

5.1. Effect of SPI content on glass-transition temperature

Fig. 2 shows the DSC thermograms depicting the glass-transition temperature (T_g) of PBA-a, SPI, and their blends. At heating rate of 10 °C/min, the T_g of the neat polybenzoxazine (PBA-a) was determined to be 160 °C. The T_gs of all blends were slightly higher than that of neat PBA-a ranging from 163 to 169 °C, while the T_g of the SPI was 173 °C. It is found that SPI was able to elevate the T_gs of the blends. In these systems, there was only one broad T_g in all blend compositions. However, the systems exhibit partial miscibility [26] as evidenced by a transformation of transparent PBA-a and SPI to opaque appearance with orange color of the blends.

Storage moduli of the PBA-a, SPI, and their blends in the temperature range of 40–220 °C are illustrated in Fig. 3. The thermograms revealed the glassy state moduli, reported at 40 °C of PBA-a to be approximately 3.1 GPa and that of SPI to be around 1.1 GPa. Therefore, the SPI is much less stiff than PBA-a due to the presence soft silicone segments in its molecular structure. The stability of the polymer can be seen from the slope of the glassy state moduli in the DMA thermograms. The lower the slope of the glassy state modulus, the greater is the thermal stability of the polymer. As a result, DMA thermograms suggested that SPI was more thermally stable than PBA-a. The presence of the SPI fraction thus helps improving thermal stability of the resulting blends.

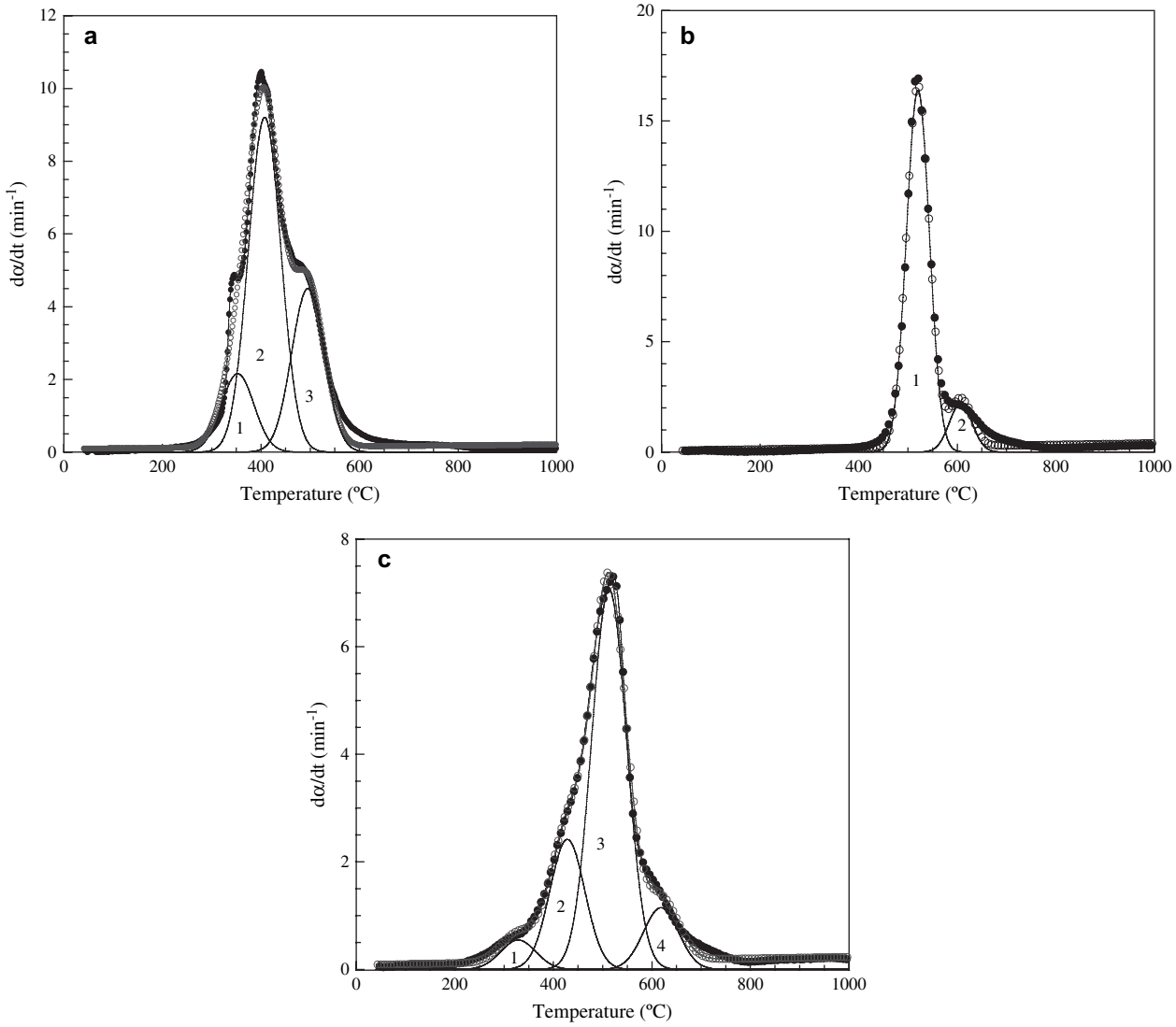

Fig. 7. DTG curve and individual contributions of (a) PBA-a (20 °C/min), $R^2 = 0.9918$; (b) SPI (20 °C/min), $R^2 = 0.9958$; (c) blends with 75 wt% of SPI (20 °C/min), $R^2 = 0.9968$; (●) experimental data, (○) simulated curve.

In addition, the tan δ of the polyimides and their blends is depicted in Fig. 4. Generally, the magnitude of tan δ peaks reflects the large scale mobility associated with α relaxation process, whereas the width of the tan δ relates to the homogeneity of the materials. The peak at lower temperature of 166 °C could be attributed to that of PBA-a and the peak at higher temperature of 184 °C was attributed to that of SPI. It can be noticed that only one single and broad peak was observed in all blend systems. Furthermore, the peaks of the blends were found to shift to higher temperature with increasing SPI content, which corresponds to the DSC results.

5.2. Thermogravimetric analysis of the blends and degradation kinetics

TGA thermograms of PBA-a, SPI, and their blends at various weight ratios of SPI are presented in Fig. 5. From the figure, it can be observed that the addition of SPI was able to enhance the decomposition temperature of the PBA-a. The inset of Fig. 5 explains the relationship between the decomposition temperatures at 10% weight loss and the SPI content in the blends. It clearly shows that the decomposition temperatures of the blends increase from about 360 °C (for 0 wt% of SPI) to about 500 °C (for 100 wt% of SPI) with the increase of the SPI fraction.

Interestingly, the char yields of the blended systems exhibited the synergistic behavior as shown in Fig. 6. The char yields of the blends were higher than those of neat PBA-a and SPI. The highest char value at 800 °C of about 45% was found at 75 wt% of the SPI fraction, while the value of pure PBA-a was only 30%. Theoretically, the possible reason for synergism in the char formation is due to a large amount of aromatic ring in the blends with some additional chemical bonding between the PBA-a and the SPI. This synergy in the char formation was also observed in the systems of polybenzoxazine alloyed with other types of polyimides [27].

From these results, we selected the blend at 75 wt% of SPI for further kinetic studies of the blending systems since it

Table 2
Initial temperature, final temperature, and peak temperature of small curves for polybenzoxazine, SPI and their blends at 20 °C/min in N_2 atmosphere

Polysiloxane-*block*-polyimide (wt% in PBA-a)										
		0			25	50	75			100
Stage 1	T_i	280	Stage 1	T_i	213	198	227	Stage 1	T_i	422
	T_{peak}	353		T_{peak}	323	313	328		T_{peak}	521
	T_f	426		T_f	432	427	429		T_f	618
	% Area	14		% Area	9	8	5		% Area	88
Stage 2	T_i	316	Stage 2	T_i	292	294	310	Stage 2	T_i	521
	T_{peak}	408		T_{peak}	420	429	428		T_{peak}	607
	T_f	499		T_f	548	563	546		T_f	694
	% Area	58		% Area	51	40	22		% Area	12
Stage 3	T_i	413	Stage 3	T_i	386	375	384	R^2		0.9958
	T_{peak}	496		T_{peak}	509	511	513			
	T_f	577		T_f	634	645	642			
	% Area	28		% Area	34	44	63			
R^2		0.9918	Stage 4	T_i	504	501	508			
				T_{peak}	609	616	618			
				T_f	714	730	728			
				% Area	6	8	10			
			R^2		0.9976	0.9974	0.9968			

Note: T_i = initial temperature and T_f = final temperature.

provides maximum char yield. After obtaining the TGA and DTG curves, we used Peakfit program to separate the DTG curves of the blends at 0 wt%, 75 wt%, and 100 wt%. After resolving the curves by using the computer software, it can be noticed that the DTG curve of the PBA-a, presented in Fig. 7a, composes of a three-stage weight-loss process. This result is in good agreement with the study of Hemvichian et al., which reports that this degradation process was observed with the middle peak having the highest maximum rate of weight loss. In addition, the degradation products were identified into eight categories as follows: benzene derivatives, amines, phenolic compounds, 2,3-benzofuran derivatives, iso-quinoline derivatives, biphenyl compounds, Mannich base compounds, and phenanthridine derivatives [3]. Moreover for the pure SPI, the DTG curve can also be resolved into two main loss processes as shown in Fig. 7b. These results correspond to the degradation study in the system of siloxane-containing polyimide with the molecular weight of 1300 [28], which reported at least two overlapping stages. Moreover, our results also reveal the same phenomenon as found in the similar system of polydimethylsiloxane (PDMS). It is well known that the thermal degradation of PDMS in nitrogen atmosphere results in depolymerization over the range of 400–650 °C to produce cyclic oligomers [29,30]. In the degradation of PDMS, the most abundant product is reported to be the trimer of hexamethylcyclotrisiloxane with decreasing amounts of tetramer, and higher oligomers [29]. For the blend system with 75 wt% of SPI as shown in Fig. 7c, the DTG can be resolved into four curves, which represent the four main stages of degradation in the blend. The determination of the areas under the resolved peaks (% area) and the peak positions (T_{peak}) was useful to make us understand more about the degradation process of the blend system. All these data including initial decomposition temperatures (T_i) and final decomposition temperatures (T_f) of pure PBA-a, SPI, and their blends are exhibited in Table 2. In comparison of peak positions, it can be observed that the T_{peak}s of stage 1 and stage 2 in the blends for all SPI compositions are similar to that of stage 1 in pure PBA-a, while the T_{peak}s of stage 4 in the blends for are close to that of stage 2 in pure SPI. Additionally, the T_{peak}s of stage 3 in the blends are the values between the T_{peak} of stage 3 in pure PBA-a and that of stage 1 in pure SPI. In the determination of the areas

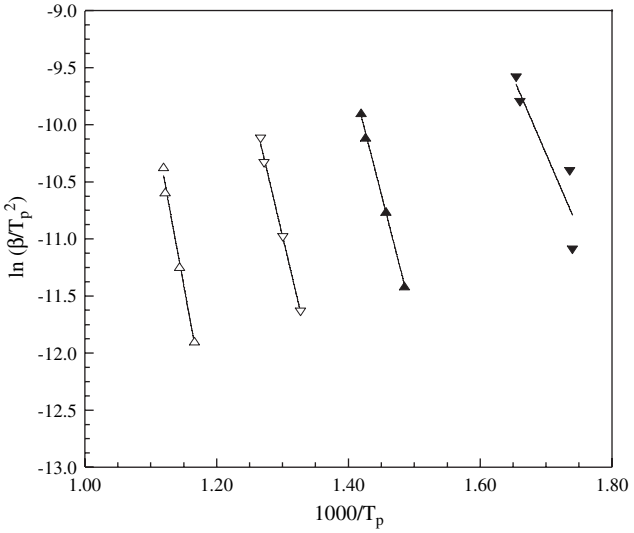

Fig. 8. Plots of $\ln \beta/T_p^2$ versus $1000/T_p$ at different heating rates according to Kissinger method for the blends (75 wt% of SPI): (▼) peak 1, (▲) peak 2, (□) peak 3, (△) peak 4.

Table 3
Activation energies obtained by using Kissinger method for the blend (75 wt% of SPI)

Peak 1		Peak 2		Peak 3		Peak 4	
E_a (kJ/mol)	R^{2a}	E_a (kJ/mol)	R^{2a}	E_a (kJ/mol)	R^{2a}	E_a (kJ/mol)	R^{2a}
111	0.9204	187	0.9983	202	0.9972	260	0.9919

[a] Correlation coefficient.

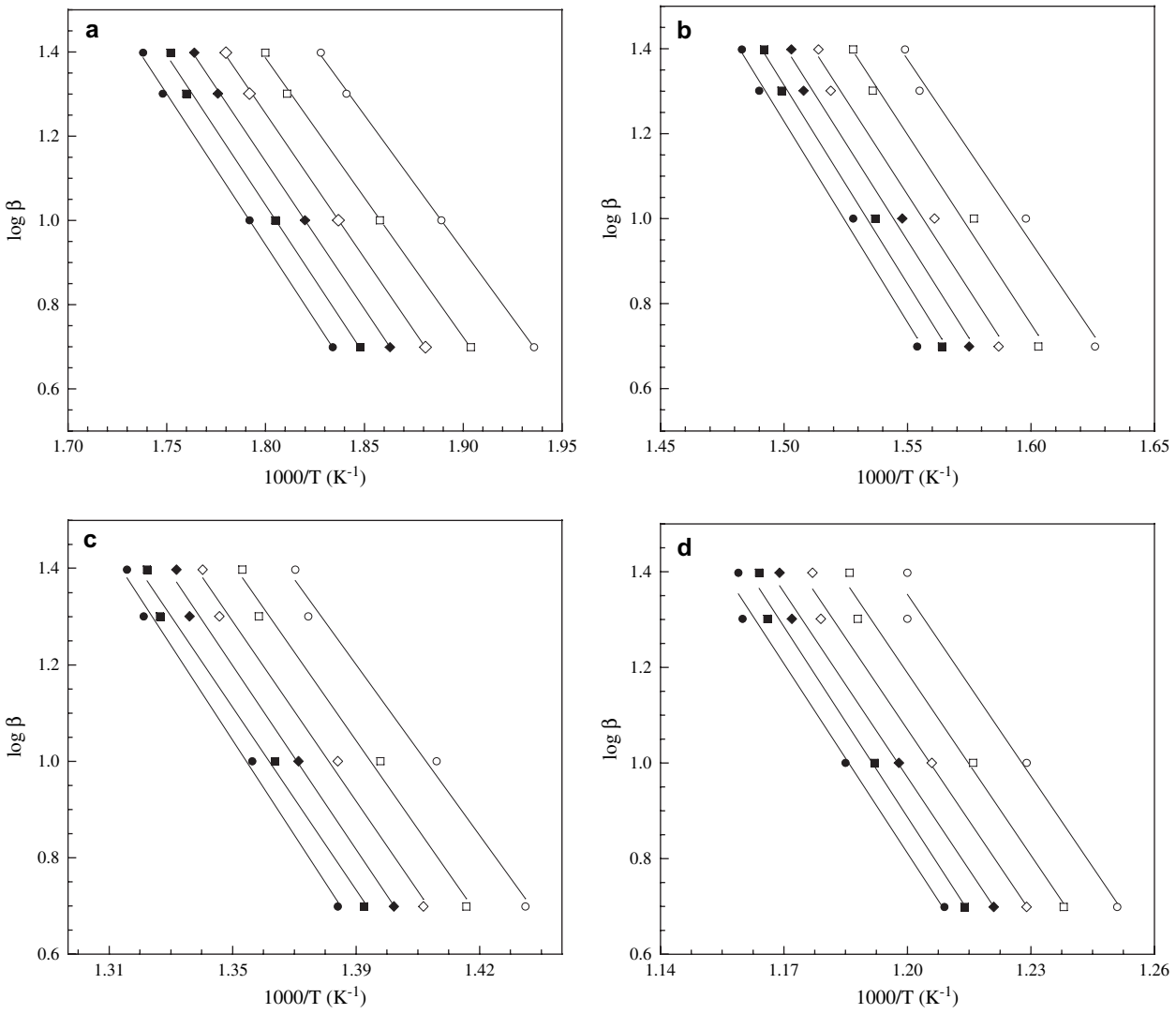

Fig. 9. Plots of log β versus 1000/T according to Flynn–Wall–Ozawa method for the blend (75 wt% of SPI) with weight loss from 5% to 20% conversion for (a) peak 1; (b) peak 2; (c) peak 3; (d) peak 4: (○) 5%, (□) 8%, (◇) 11%, (◆) 14%, (■) 17%, and (●) 20%.

under the resolved curves, the values of all degradation stages of the blends are related to the contents of PBA-a and SPI. It can be seen that the addition of SPI led to the decrease of the % area values in stages 1 and 2 and the increase of the values in stages 3 and 4. These results confirm that that stages 1 and 2 of the degradation in the blends are mainly from the degradation of PBA-a, while stage 4 of the degradation in the blends is from the degradation of SPI. For the stage 3 of degradation, it is proposed to be the degradation of some additional chemical bonding between the PBA-a and the SPI.

After the four overlapped curves were resolved, the conversions were calculated from the areas under the curves by using Simpson's 3/8 rule. Then, the E_a of each one was obtained via three mentioned methods.

5.3. Calculation of the thermal degradation kinetics parameters

The E_a of the thermal degradation process of this blend was determined using three well-known methods for dynamic heating experiment i.e., the Kissinger method, Flynn–Wall–Ozawa method, and Coats–Redfern method.

By using Kissinger method, the E_a can be calculated from the slope of the plot of $\ln(\beta/T_p^2)$ versus $1000/T_p$ (T_p is the temperature at the maximum weight-loss rate) as presented in Fig. 8. The calculated values are shown in Table 3. The obtained E_a values of stages 1, 2, 3, and 4 are 111, 187, 202, 260 kJ/mol, respectively. From the literature [12,31], the Kissinger's method was reported to provide highly reliable values of E_a with an error of less than 5% independent of reaction mechanism, provided that $E/RT > 10$.

The E_a of the blends can also be determined using the method of Flynn–Wall–Ozawa from a linear fitting of ln β versus 1000/T at different conversions (Fig. 9a–d). Owing to the fact that this equation was derived using the Doyle approximation only conversion values in the low range can be used. In this study, the conversion values of 5%, 8%, 11%, 14%, 17%, and 20% were used. Fig. 9a–d shows that the fitting straight lines are nearly parallel. Using Flynn–Wall–Ozawa method, the E_a values corresponding to the different conversions are listed in Table 4. The

Table 4
Activation energies obtained by using Flynn–Wall–Ozawa method for the blend (75 wt% of SPI)

Conversion (%)	E_a (kJ/mol)	R^{2a}	E_a (kJ/mol)	R^{2a}
	Peak 1		Peak 2	
5	117	0.9996	157	0.9895
8	120	0.9992	161	0.9905
11	125	0.9996	164	0.9882
14	127	0.9996	168	0.9917
17	130	0.9970	170	0.9935
20	130	0.9985	173	0.9933
Average	125		166	
	Peak 3		Peak 4	
5	172	0.9900	231	0.9856
8	178	0.9940	231	0.9904
11	181	0.9928	233	0.9912
14	186	0.9954	236	0.9943
17	184	0.9925	239	0.9909
20	190	0.9946	241	0.9898
Average	182		235	

[a] Correlation coefficient.

calculated E_a from this method are 125, 166, 182, and 235 kJ/mol for peaks 1, 2, 3, and 4, respectively.

The method by Coats–Redfern is one of the most widely used procedure for the determination of the reaction processes [10,19,21]. From Eq. (9), proposed by Coats and Redfern, the E_a for all $g(\alpha)$ functions listed in Table 1 can be obtained at constant heating rate. In this study, the same conversion values have been used as those used in the Flynn–Wall–Ozawa methods. Table 5 shows E_a, A, and correlations for conversions in the range 5–20% at constant heating rate of 20 °C/min. It was found that the solid state thermal degradation mechanism of the blends with 75 wt% of SPI is likely to be of F1 type, because this mechanism presents the E_a that is similar to the value obtained by isoconvensional methods. Furthermore in comparison with other mechanisms, this mechanism renders the lowest E_a to start the degradation stage [32]. The type of degradation mechanism is confirmed by Criado method in the next determination.

As presented in Table 6, Coats–Redfern method was applied at the heating rate of 25, 20, 10, and 5 °C/min to determine the average values of the E_a, A, and the degradation mechanism. The E_a calculated by Coats–Redfern method are 116, 174, 223, and 281 kJ/mol. It is clearly shown that the E_a of each degradation stage increases with the increase of the heating rates. In addition, the results suggest F1 type of solid state thermal degradation mechanism for all four stages and all heating rates. The possible reason that the increase of the amount of SPI led to the increase of area under the curve of stage 3 of the blends is that stage 3 correlates with SPI structure. The E_a of this peak was around 218 kJ/mol, which was lower than the bond dissociation energy of Si–C bond (360 kJ/mol), the weakest bond of the base polymers [33]. Hence, the decomposition of the blends could be governed mainly by the molecular structure and kinetic consideration and not by bond energies for stage 3.

By using Coats–Redfern method, the calculated E_a at 20 °C of PBA-a for stages 1, 2, and 3 are 172, 209, and

Table 5
Activation energies obtained by using Coats–Redfern method for several solid state processes at a heating rate of 20 °C/min for the blend (75 wt% of SPI)

Type	E_a (kJ/mol)	ln A (min^{-1})	R^2	Type	E_a (kJ/mol)	ln A (min^{-1})	R^2
Peak 1				Peak 2			
A2	57	10.46	0.9976	A2	82	13.07	0.9976
A3	35	5.55	0.9971	A3	51	7.31	0.9972
A4	24	2.95	0.9965	A4	35	4.30	0.9967
R1	116	22.76	0.9971	R1	164	27.67	0.9971
R2	120	22.93	0.9976	R2	169	27.97	0.9975
R3	121	22.82	0.9977	R3	171	27.90	0.9976
D1	247	48.78	0.9974	D1	339	58.15	0.9973
D2	247	48.78	0.9976	D2	346	58.75	0.9975
D3	252	48.43	0.9979	D3	353	58.58	0.9978
D4	249	47.66	0.9977	D4	348	57.69	0.9976
F1	124	24.50	0.9980	F1	174	29.68	0.9979
F2	6	−1.64	0.8542	F2	10	−0.88	0.9040
F3	21	3.05	0.9470	F3	31	4.23	0.9561
Peak 3				Peak 4			
A2	105	15.23	0.9975	A2	139	34.94	0.9976
A3	66	8.76	0.9972	A3	88	34.48	0.9973
A4	47	5.41	0.9968	A4	63	34.14	0.9969
R1	210	31.70	0.9970	R1	275	35.62	0.9969
R2	217	32.14	0.9975	R2	284	35.65	0.9974
R3	219	32.11	0.9976	R3	287	35.66	0.9975
D1	432	66.21	0.9972	D1	565	36.34	0.9971
D2	441	66.99	0.9975	D2	576	36.36	0.9974
D3	450	66.99	0.9770	D3	588	36.38	0.9977
D4	444	65.99	0.9976	D4	580	36.36	0.9975
F1	223	33.98	0.9978	F1	293	35.68	0.9978
F2	15	−0.20	0.9245	F2	22	33.08	0.9347
F3	42	5.38	0.9603	F3	57	34.05	0.9613

Table 6
Average activation energies obtained by using Coats–Redfern method at 25, 20, 10, 5 °C/min for the blend (75 wt% of SPI)

Heating rate (°C/min)	E_a (kJ/mol)	ln A (min^{-1})	Possible mechanism
Peak 1			
5	113	23.35	F1
10	108	22.21	F1
20	124	24.50	F1
25	119	23.87	F1
Average	116		
Peak 2			
5	161	28.51	F1
10	168	29.10	F1
20	174	29.68	F1
25	175	28.51	F1
Average	170		
Peak 3			
5	206	32.66	F1
10	217	34.14	F1
20	223	33.98	F1
25	252	39.25	F1
Average	225		
Peak 4			
5	287	39.73	F1
10	272	37.24	F1
20	293	35.68	F1
25	270	36.12	F1
Average	281		

263 kJ/mol, respectively (Table 7). The solid state thermal degradation mechanism of PBA-a is proposed to be of F1 type. The PBA-a thermal degradation of this study is in agreement with the results in the literature [34], which reveals the phenolic cleavage at the maximum derivative of peak temperature at around 400 °C.

With the Coats–Redfern method, the calculated E_a at 20 °C of neat SPI for peaks 1 and 2 are 369 and 460 kJ/mol, respectively (Table 8). These calculation results coincide with the bonding energy of Si–C (360 kJ/mol) [33], the weakest bond in PDMS, and that of Si–O (454 kJ/mol) [35]. Hence, the degradation of SPI could possibly be governed mainly by the breaking of Si–C bond and Si–O bond.

Table 8
Activation energies obtained by using Coats–Redfern method for several solid state processes at a heating rate of 20 °C/min of BSF30

Type	Peak 1			Peak 2		
	E_a (kJ/mol)	ln A (min^{-1})	R^2	E_a (kJ/mol)	ln A (min^{-1})	R^2
A2	178	26.64	0.9959	223	30.14	0.9957
A3	115	16.55	0.9956	144	18.89	0.9955
A4	83	11.40	0.9952	104	13.16	0.9951
R1	348	52.80	0.9953	434	59.44	0.9952
R2	358	53.85	0.9958	447	60.66	0.9956
R3	362	54.04	0.9959	452	60.90	0.9958
D1	708	107.96	0.9954	882	121.23	0.9953
D2	722	109.54	0.9958	899	123.04	0.9956
D3	737	110.39	0.9961	917	124.10	0.9959
D4	727	108.82	0.9952	905	122.38	0.9957
F1	369	56.33	0.9962	460	63.30	0.9960
F2	31	3.03	0.9502	40	3.73	0.9569
F3	76	10.99	0.9648	94	12.33	0.9684

From the calculation in the system of SPI, the solid state thermal degradation mechanism is proposed to be of F1 type. In this study, the degradation phenomenon of SPI coincides with that of the literature [35], which reported that the thermal degradation of PDMS in inert atmosphere results in degradation over the range of 400–650 °C.

In comparison of PBA-a, SPI and the blend with 75 wt% of SPI, the E_a of the blend was found to be lower than those of both pure components. This phenomenon corresponds to the research of Nandan et al. [36], who studied the blending system of poly(ether ether ketone)/poly(aryl ether sulphone). They reported that the E_a of the blends were lower than that of the pure components because of different factors that concurrently effect the process of degradation. Firstly, interactions are possible among the different components in the blend during degradation and among the products of degradation. These chemical reactions can lead to an acceleration of the degradation rate with respect to that of pure components. These reactions can be grouped into following processes [37,38].

– Reactions between macromolecules and small molecules,
– reactions between macromolcules and small radicals,

Table 7
Activation energies obtained by using Coats–Redfern method for several solid state processes at a heating rate of 20 °C/min of BA-a

Type	Peak 1			Peak 2			Peak 3		
	E_a (kJ/mol)	ln A (min^{-1})	R^2	E_a (kJ/mol)	ln A (min^{-1})	R^2	E_a (kJ/mol)	ln A (min^{-1})	R^2
A2	81	14.82	0.9969	99	16.67	0.9969	126	19.13	0.9970
A3	51	8.55	0.9964	62	9.80	0.9965	80	11.45	0.9966
A4	36	5.29	0.9959	44	6.24	0.9960	57	7.49	0.9962
R1	162	30.76	0.9964	196	34.27	0.9964	248	38.89	0.9963
R2	167	31.16	0.9969	202	34.76	0.9968	256	39.52	0.9968
R3	169	31.12	0.9970	204	34.75	0.9970	258	39.56	0.9970
D1	333	64.13	0.9966	403	71.15	0.9966	508	80.38	0.9965
D2	340	64.86	0.9969	411	71.99	0.9969	518	81.41	0.9968
D3	347	64.82	0.9972	420	72.07	0.9971	529	81.68	0.9971
D4	342	63.84	0.9970	414	71.01	0.9970	522	80.50	0.9969
F1	172	32.97	0.9972	209	36.66	0.9972	263	41.56	0.9972
F2	11	−0.17	0.9191	14	0.24	0.9283	19	0.91	0.9348
F3	32	5.28	0.9587	39	6.00	0.9606	51	7.22	0.9606

– reactions between macroradicals and small molecules,
– reactions between two small molecules,
– reaction between two macroradicals,
– reaction between macromolecules and macroradicals.

In addition, reactions with small molecules or small radicals can give rise to faster breakage of the macromolecules and to chemical structures that act as stabilizer groups.

These above reasons can explain the phenomenon that the E_a of the blends in many systems [38–40] are not close to the predicted values on the basis of linear additive behaviour, using following equation,

$$E_a = E_{a1}w_1 + E_{a2}w_2 \quad (15)$$

where E_{a1} and E_{a2} are activation energies of the homopolymers, and w_1 and w_2 are the weight fraction of components 1 and 2, respectively [36].

5.4. Determination of the reaction mechanism using Criado method

The $Z(\alpha)-\alpha$ master curves can be plotted using Eq. (13) according to different reaction mechanisms shown in Table 1. The experimental data at 20 °C/min obtained by Flynn–Wall–Ozawa method (Table 4) were substituted into Eq. (14). Fig. 10a–d shows the $Z(\alpha)-\alpha$ master and experimental curve of the blend with 75 wt% of PSI. The results show that the experimental curves of all four steps of degradation belong to F1 reaction mechanism (random nucleation having one nucleus on individual particle) with rate-controlling step of the nucleation process. Figs. 11a–c and 12a,b exhibit the comparison of the experimental curves of pure PBA-a and PSI, respectively. It can be observed that the degradation of pure PBA-a and PSI was proved to obey the F1 mechanism. That means random nucleation with one nucleus on the individual particle. The degradation

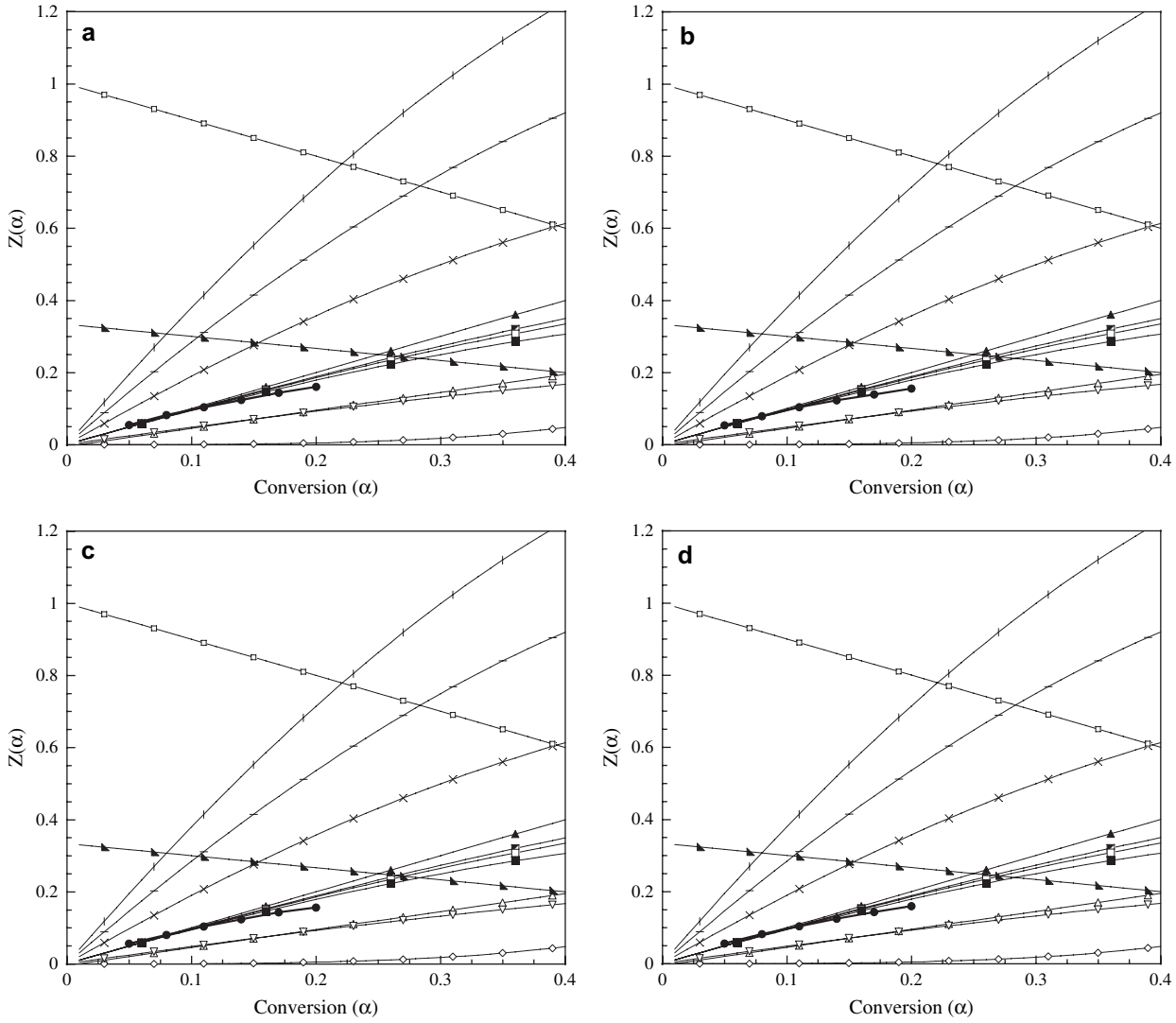

Fig. 10. Plots of $Z(\alpha)$ versus α of the blend (75 wt% of SPI) compared between experimental curve and master curve at different mechanisms for (a) peak 1; (b) peak 2; (c) peak 3; (d) peak 4: (×) A2, (|) A3, (–) A4, (▲) R1, (◩) R2, (□) R3, (△) D1, (◇) D2, (▽) D3, (◆) D4, (■) F1, (▫) F2, (◣) F3, (●) experimental data.

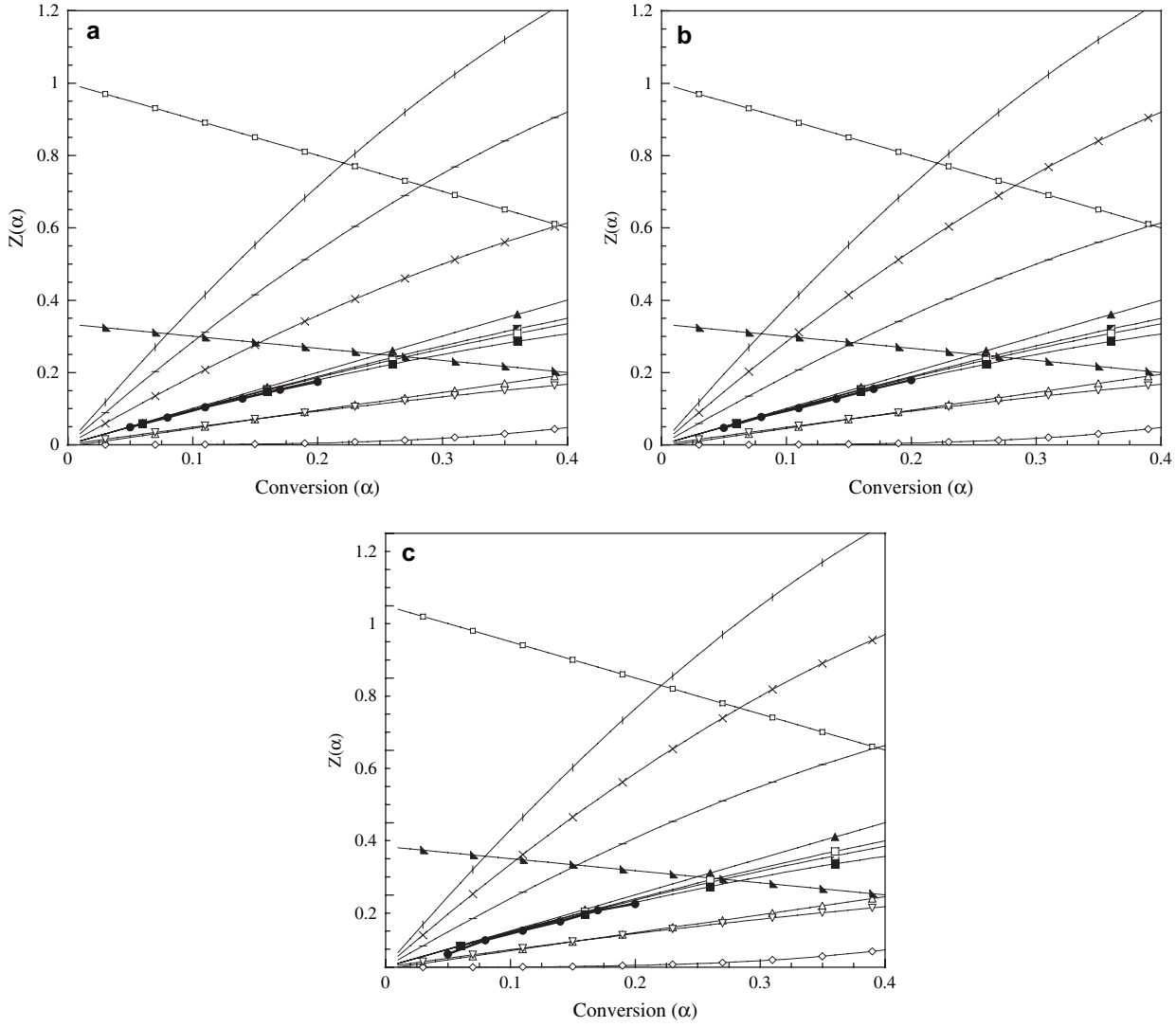

Fig. 11. Plots of $Z(\alpha)$ versus α of PBA-a compared between experimental curve and master curve at different mechanisms for (a) peak 1; (b) peak 2; (c) peak 3; (d) peak 4: (×) A2, (|) A3, (–) A4, (▲) R1, (◩) R2, (□) R3, (△) D1, (◇) D2, (▽) D3, (◆) D4, (■) F1, (▫) F2, (◣) F3, (●) experimental data.

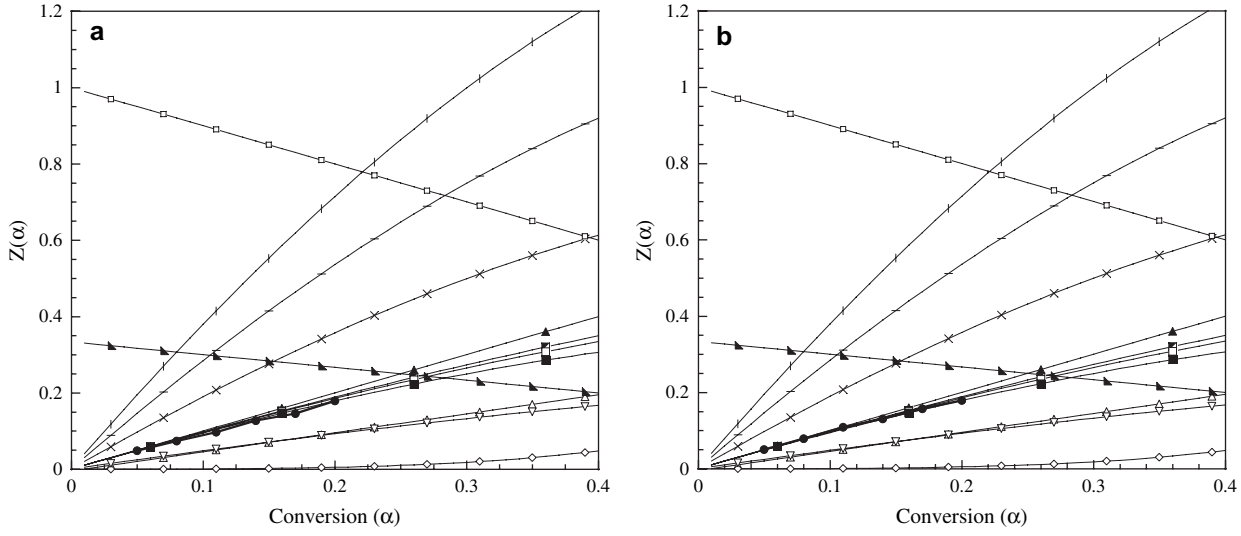

Fig. 12. Plots of $Z(\alpha)$ versus α of BSF30 compared between experimental curve and master curve at different mechanisms for (a) peak 1; (b) peak 2: (×) A2, (|) A3, (–) A4, (▲) R1, (◩) R2, (□) R3, (△) D1, (◇) D2, (▽) D3, (◆) D4, (■) F1, (▫) F2, (◣) F3, (●) experimental data.

was initiated from one random point acting as growth center, which follows unimolecular decay law with first order reaction [41,42].

6. Conclusions

In the blending systems of BA-a monomer and SPI, synergistic behavior of char yield was observed. The possible reason for the increase of char yield is that there was higher cross-link density in the blend than both neat polybenzoxazine and SPI. PBA-a and SPI showed three-stage weight-loss process and two-stage weight-loss process, respectively. The degradation of the blends between benzoxazine monomer and SPI was found to be a complex process composed of at least four overlapping stages, of which the E_a can be calculated. The study of separated curves from Criado method indicates that PBA-a, SPI and their blending systems follow F1 thermal degradation mechanism in the conversion range considered.

Acknowledgements

The authors would like to thank the Thailand Research Fund (TRF) and the Commission on Higher Education for the financial support through the Research Grant for Mid-Career University Faculty of fiscal year 2005–2007. The present research receives partial financial support from the Foundation for the International Exchange of the Faculty of Engineering, Tokyo Institute of Technology. In addition, CU Graduate Thesis Grant of Chulalongkorn University is also acknowledged. Additionally, the authors would like to thank Mettler-Toledo (Thailand) Co., Ltd. for the kind support in the use of thermogravimetric analysis.

References

[1] Ishida H. US Patent 5,543,516; 1996.
[2] Nair CPR. Advances in addition-cure phenolic resins. Prog Polym Sci 2004;29:401–98.
[3] Hemvichian K, Ishida H. Thermal decomposition process in aromatic amine-based polybenzoxazine investigated by TGA and GC–MS. Polymer 2002;43:4391–402.
[4] Takeichi T, Agag T, Zeidam R. Preparation and properties of polybenzoxazine/poly(imide siloxane) alloys: in situ ring-opening polymerization of benzoxazine in the presence of soluble poly(imide-siloxane)s. J Polym Sci Part A Polym Chem 2001;39:2633–41.
[5] Agag T, Takeichi T. Polybenzoxazine–montmorillonite hybrid nanocomposites: synthesis and characterization. Polymer 2000;41:7083–90.
[6] Agag T, Takeichi T. Synthesis and properties of silica-modified polybenzoxazine. Mater Sci Forum 2004;449–452:1157–60.
[7] Furukawa N, Yamada Y, Kimura Y. Preparation and stress relaxation properties of thermoplastic polysiloxane-*block*-polyimides. High Perform Polym 1996;8:617–30.
[8] Yamada Y. Siloxane modified polyimides for microelectronics coating applications. High Perform Polym 1998;10:69–80.
[9] Furukawa N, Yuasa M, Kimura Y. Structure analysis of a soluble polysiloxane-*block*-polyimide and kinetic analysis of the solution imidization of the relavant polyamic acid. J Polym Sci Part A Polym Chem 1998;36:2237–45.
[10] Coats AW, Redfern JP. Kinetic parameters from thermogravimetric data. Nature 1964;201:68–9.
[11] Nam JD, Seferis JC. A composition methodology for multistage degradation of polymers. J Polym Sci Part B Polym Phys 1991;30:601–8.
[12] Barral L, Cano J, Lopez J, Lopez-Bueno I, Nogueira P, Ramirez C, et al. Thermogravimetric study of tetrafunctional/phenol novolac epoxy mixtures cured with a diamine. J Therm Anal Calorim 1998;51:489–501.
[13] Kissinger HE. Reaction kinetics in differential thermal analysis. Anal Chem 1957;29:1702–6.
[14] Ozawa T. A new method of analyzing thermogravimetric data. Bull Chem Soc Jpn 1965;38:1881–6.
[15] Liaw DJ, Shen WC. Curing of acrylated epoxy-resin based on bisphenols. Polym Eng Sci 1994;34:1297–303.
[16] Nam JD, Seferis JC. Generalized composite degradation kinetics for polymeric systems under isothermal and nonisothermal conditions. J Polym Sci Part B Polym Phys 1992;30:455–63.
[17] Flynn JH. The 'temperature integral' – its use and abuse. Thermochim Acta 1997;300:83–92.
[18] Doyle CD. Kinetic analysis of thermogravimetric data. J Appl Polym Sci 1961;5:285–92.
[19] Criado JM, Malek J, Ortega A. Applicability of the master plots in kinetic analysis of a non-isothermal rate. Thermochim Acta 1989;147:377–85.
[20] Criado JM, Perez-Maqueda LA, Gotor FJ, Malek J, Koga N. A unified theory for the kinetic analysis of solid state reactions under any thermal pathway. J Therm Anal Calorim 2003;72:901–6.
[21] Pérez-Maqueda LA, Criado JM, Gotor FJ, Malek J. Advantages of combined kinetic analysis of experimental data obtained under any heating profile. J Phys Chem A 2002;106:2862–8.
[22] Paterson WL. Computation of the exponential trap population integral of glow curve theory. J Comput Phys 1971;7(1):187–90.
[23] Pérez-Maqueda LA, Criado JM. The accuracy of Senum and Yang's approximations to the Arrhenius integral. J Therm Anal Calorim 2000;60:909–15.
[24] Urbanovici E, Popescu C, Seqal E. Improved iterative version of the Coats–Redfern method to evaluate non-isothermal kinetic parameters. J Therm Anal Calorim 1999;58:683–700.
[25] Low HY, Ishida H. Structural effects of phenols on the thermal and thermo-oxidative degradation of polybenzoxazines. Polymer 1999;40:4365–76.
[26] Sperling LH, Hu R. In: Utracki LA, editor. Polymer blends handbook, vol. 1; 2002. p. 426.
[27] Takeichi T, Guo Y, Rimdusit S. Performance improvement of polybenzoxazine by alloying with polyimide: effect of preparation method on the properties. Polymer 2005;46:4909–16.
[28] Chang TC, Wu KH, Liao CL, Lin ST, Wang GP. Thermo-oxidative degradation of siloxane-containing polyimide and unmodified polyimide. Polym Degrad Stab 1998;62:299–305.
[29] Thomas TH, Kendrick TC. Thermal analysis of polydimethylsiloxanes. I. Thermal degradation in controlled atmospheres. J Polym Sci 1969;7:537–49.
[30] Grassie N, MacFarlane IG. The thermal degradation of polysiloxanes [polydimethylsiloxane]. Eur Polym J 1978;14:875–84.
[31] Criado JM, Ortega A. Non-isothermal transformation kinetics: remarks on the Kissinger method. J Non-Cryst Solids 1986;87:302–11.
[32] Albano C, Freitas ED. Thermogravimetric evaluation of the kinetics of decomposition of polyolefin blends. Polym Degrad Stab 1998;61:289–95.
[33] Korshak VV. The chemical structure and thermal characteristics of polymers. Jerusalem: Keter Press; 1971.
[34] Hemvichian K, Kim DH, Ishida H. Identification of volatile products and determination of thermal degradation mechanisms of polybenzoxazine model oligomers by GC–MS. Polym Degrad Stab 2005;87:213–24.
[35] Camino G, Lomakin SM, Lazzari M. Polydimethylsiloxane thermal degradation. Part 1. Kinetic aspects. Polymer 2001;42:2395–402.
[36] Nandan B, Kandpal LD, Mathur GN. Poly(ether ether ketone)/poly(aryl ether sulphone) blends: thermal degradation behaviour. Eur Polym J 2003;39:193–8.
[37] Hamid SH, Amin MB, Maadhah AG. Handbook of polymer degradation. New York: Marcel Dekker; 1992.

[38] Remiro PM, Cortazar MM, Calahorra ME. A study of the degradation of uncured DGEBA/PVP blends by thermogravimetry and their miscibility state. J Mater Sci 1999;34:2627–33.
[39] Erceg M, Kovacic T, Klaric I. Dynamic thermogravimetric degradation of poly(3-hydroxybutyrate)/aliphatic-aromatic copolyester blends. Polym Degrad Stab 2005;90:86–94.
[40] Mohanty S, Mukunda PG, Nando GB. Kinetics of thermal degradation and related changes in the structure of blends of poly(ethylene-*co*-acrylic acid) (PEA) and epoxidized natural rubber (ENR). Polym Degrad Stab 1996;52:235–44.
[41] Moguet F, Bordére S, Tressaud A, Rouquerol F, Llewellyn P. Deintercalation process of fluorinated carbon fibres – II. Kinetic study and reaction mechanisms. Carbon 1998;36:1199–205.
[42] Dinh LN, Cecala CM, Leckey JH, Balooch M. The effects of moisture on LiD single crystals studied by temperature-programmed decomposition. J Nucl Mater 2001;295:193–204.